

Water near lipid membranes as seen by infrared spectroscopy

Hans Binder

Received: 6 July 2006 / Revised: 2 October 2006 / Accepted: 10 October 2006 / Published online: 7 November 2006
© EBSA 2006

Abstract The ordering and H-bonding characteristics of the hydration water of the lipid 1-palmitoyl-2-oleoylphosphatidylcholine (POPC) were studied using polarized infrared spectroscopy by varying either the temperature or the relative humidity of the ambient atmosphere of multilayer samples. The OH-stretching band of lipid-bound water was interpreted by a simplified two-state model of well-structured, low density “network” water and of less-structured dense “multimer” water. The IR-spectroscopic data reflect a rather continuous change of the water properties with increasing distance from the membrane and with changing temperature. Network and multimer water distribute across the whole polar interphase with changing composition and orientation. Upon dehydration the fraction of network water increases from about 30 to 60%, a value which is similar to that in supercooled water at -25°C . The highly ordered gel phase gives rise to an increased fraction of structured network water compared with the liquid crystalline phase. The IR order parameter shows that the water dipoles rearrange from a more parallel towards a more perpendicular orientation with respect to the membrane normal with progressive hydration.

Keywords Lipid hydration · Water structure · Hydrogen bonding · Infrared spectroscopy · Humidity-titration technique

Introduction

The structure of water surrounding lipid bilayer-membranes has been studied by a wide variety of techniques and is considered a paradigm for biomembrane hydration. Lipid hydration is of great importance in studies of the phase behavior of lipid/water systems and not least in studies of the repulsive hydration forces between lipid bilayers (Binder 2003; Gawrisch et al. 1992; Le Neveu et al. 1976; Leikin and Parsegian 1993; Parsegian and Rand 1991; Rand and Parsegian 1989). Studies on lipid hydration have been pioneered by a number of investigators who use gravimetric sorption experiments (Jendrasiak and Hasty 1974), scattering methods (Büldt et al. 1979; Le Neveu et al. 1976; Luzzati 1968) and NMR spectroscopy (Finer and Darke 1974; Seelig 1977) as the basic techniques. Among these pioneers is Klaus Arnold, who initiated intensive investigations on phospholipid/water mixed systems in the Molecular NMR (later Biomembrane physics) group at the University of Leipzig in the mid-1970s. These studies revealed new insights into the properties of hydration water of phospholipids using ^{31}P - and ^2H -NMR spectroscopy (Arnold et al. 1981, 1983; Gawrisch et al. 1985; Klose et al. 1985) and also quantum chemical calculations and computer simulations (Frischleder et al. 1977; Peinel et al. 1983a, b).

It was found that the arrangement of the lipid headgroups “perturbs” the ordering and the dynamics of water molecules compared with the properties of

Dedicated to Prof. K. Arnold on the occasion of his 65th birthday.

H. Binder (✉)
Interdisciplinary Centre for Bioinformatics,
University of Leipzig, Haertelstr. 16-18,
04107 Leipzig, Germany
e-mail: binder@izbi.uni-leipzig.de

bulk water. For example, this perturbed water gives rise to a typical quadrupole splitting of the ^2H -NMR spectrum if the lipids are hydrated with heavy water (Arnold et al. 1983; Finer and Darke 1974). The change of the splitting width with the hydration degree indicated that the first five water molecules added to the lipid (dipalmitoylphosphatidylcholine in this particular case) form a sort of inner hydration “shell” possessing a much larger splitting width than additional, ambient water. Parallel theoretical investigations have shown that the arrangement of water with respect to the polar interface is more adequately described using a layered geometry than a central-symmetric arrangement in hydration “shells” (Klose et al. 1985). The concept of different types of perturbed water which arrange in different layers has been commonly accepted in describing the hydration of lipid membranes. In this paper we will use the termini hydration- “shell” and “layer” as synonyms.

The primary hydration shell of surface-adsorbed water differs from the subsequent layers of water which are surrounded by other waters because the polar surface strongly interacts with this first layer of water molecules via relatively strong water-substrate (solvent–solute) interactions. Israelachvili and Wennerström assumed that the properties of the water beyond the primary hydration layer are essentially the same as those of bulk water and thus there are virtually no further hydration layers of structured water except the first one (Israelachvili and Wennerström 1996). As a consequence they suggested that the short-range repulsion between approaching membrane surfaces is caused by the entropy loss due to the confinement of thermally mobile surface groups and not from any type of structured water in the hydration shell beyond the primary layer. Methods which are sensitive to subtle changes of the water structure and interactions are required to study the question to what extent the molecular arrangement of hydration water in the vicinity of lipid membranes is affected by the polar surface.

Vibrational spectroscopy constitutes a well-proven method which is capable to characterize water properties on the molecular level. Owing to its sensitivity to the strength and arrangement of chemical bonds this method was applied to study details of the network of H-bonds in pure water and ice (Bertie and Whalley 1964a, b; Walrafen 1967, 1971). In the context of lipid hydration vibrational spectroscopy was extensively used to characterize the hydration sites of lipids (Arrondo et al. 1984; Binder 2003; Blume et al. 1988; Casal and Mantsch 1984; Dluhy et al. 1985; Pohle et al. 1998; Ter-Minassian-Saraga et al. 1988) and the properties of water which directly binds to the headgroups (Binder

et al. 1997; Grdadolnik et al. 1991; Kint et al. 1992). Correlations between the behavior of spectral bands due to vibrations of the lipid headgroup and that of the water allowed to identify the acceptor-sites for the H-bonds between the water and lipids under different conditions (see, e.g., Binder and Pohle 2000).

In addition to the characterization of the interaction pattern, infrared spectroscopy with polarized light on macroscopically aligned membranes is a well-suited method for the study of water orientation and ordering (Fringeli et al. 1972). For example, this IR linear dichroism technique revealed that water strongly orients upon binding to crystalline lipids at low hydration degrees (Binder et al. 1998; Binder and Pohle 2000). IR spectroscopy provides the ensemble average, i.e. a sort of static “snapshot” of the water arrangement owing to its characteristic time in the picosecond range. Contrarily, the NMR spectra include also dynamic averaging and thus they reflect the different time-scales of the diffusion of water near the membrane. This way both methods complement each other in their ability to detect different facets of the perturbation of water behavior bound to lipid assemblies.

Several aspects of lipid hydration continue to attract theoretical and experimental research until today (see, e.g., Milhaud 2004 for a review). Despite this extensive work, experimental data about the structure of water and the network of hydrogen bonds at the polar interface of lipid membranes are relatively rare. This interface is more like an “interphase” connecting the hydrophobic core of the lipid bilayer and the “unperturbed” bulk water. Owing to their small size, water molecules tightly fit into the free volumes of the bilayer forming malleable clusters of waters in a complex network of H-bonds which include also the phosphate and carbonyl groups of the lipid. Molecular dynamics computer simulations, for example, have shown that water effectively connects neighboring headgroups via chain-like “water bridges” (Pasenkiewicz-Gierula et al. 1999, 2000). Recent simulations analyzed the H-bonding architecture of the polar interphase and the consequences for the energetics, dynamics, macroscopic orientation and charge distribution and of perturbed water (Bhide and Berkowitz 2005; Yegiazaryan et al. 2006).

The network of H-bonds and also dipolar interactions between water and the zwitterionic lipid headgroups (Gawrisch et al. 1992) affect the structure of water and of the lipid as well because the Gibbs free energy of the whole system tends to become minimized in thermodynamic equilibrium. Hence, the control and exact adjustment of the thermodynamic state of the water in experiments on amphiphilic systems repre-

sents one important prerequisite for the unambiguous characterization of their hydration properties. Parsegian and coworkers developed the method of polymer-controlled osmotic stress adjustment to control the hydration degree in the samples in terms of an intensive thermodynamic parameter (Le Neveu et al. 1976). More than 20 years ago Arnold et al. (1983) adapted this technique to NMR-studies of lipid hydration in the presence of polyethylene glycol. This idea was further developed to the so-called humidity-titration technique, an elaborated humidity-controlled hydration pressure adjustment, which allows the effective and detailed study of the hydration properties of amphiphilic assemblies (see Ref. Binder 2003 for an overview).

The present work combines infrared (IR) spectroscopy with the humidity-titration technique to characterize the water bound to phosphatidylcholine lipid bilayers as a function of the hydration degree and temperature. Due to the time resolution of IR absorption and its sensitivity to subtle changes of chemical bonding we aim at resolving important structural and energetic properties of interfacial water in its particular H-bonded structure and at comparing these results with that predicted by computer simulations. The analysis focuses on the most prominent feature of the IR spectrum of water formed by the O–H stretching band in the spectral range 3,600–3,100 cm^{-1} . It will be demonstrated that this broad, relatively structureless region provides valuable insights into water structure and, orientation near the lipid bilayer.

Materials and methods

Sample preparation, ATR infrared measurements and spectral analysis

The lipid, 1-palmitoyl-2-oleoyl-sn-glycero-3-phosphocholine (POPC) was purchased from Avanti Polar Lipids, Inc. (Alabaster, AL, USA). Appropriate amounts of a stock solution of the lipid in methanol were spread on the surface of a ZnSe-attenuated total reflection (ATR) crystal (angle of incidence: 45°, six active reflections). The solvent evaporates under a stream of nitrogen gas within a few minutes. The lipid arranges spontaneously into macroscopically oriented multibilayer stacks which align parallel on the ATR surface. Polarized infrared (IR) absorption spectra, $A_{\parallel}(\nu)$ and $A_{\perp}(\nu)$, were recorded with light polarized parallel and perpendicular with respect to the plane of incidence using a BioRad FTS-60a Fourier transform

infrared spectrometer (Digilab, MA, USA) equipped with a wire grid polarizer. Band positions were analyzed by means of their center of gravity (COG) in the weighted sum spectrum, $A(\nu) = A_{\parallel}(\nu) + 2.55A_{\perp}(\nu)$.

The IR order parameter of an absorption band was calculated from the dichroic ratio of the baseline-corrected polarized absorbances, $R_D = A_{\parallel}/A_{\perp}$ using Harricks thick film approximation (Harrick 1967) (see also Ref. Binder and Schmiedel 1999 for details): $S_{\text{IR}} = (R_D - 2)/(R_D + 2.55)$. It is defined as the mean second order Legendre polynomial, $S_{\text{IR}} \equiv \langle 0.5(3\cos^2\theta - 1) \rangle$, where θ is the angle between the respective transition moment and the ATR normal.

Sample conditioning: the humidity-titration technique

The hydration degree of the lipid film was adjusted by means of the humidity-titration technique which “injects” water vapor in definite portions of the relative humidity (RH) into the ambient atmosphere of the lipid sample. In particular, high purity nitrogen gas of a definite RH was blown through the sample chamber. The temperature (T) and RH were adjusted by means of a flowing water thermostat (Julabo, Seelbach, Germany) and a moisture generator (HumiVar, Leipzig, Germany) with an accuracy of ± 0.05 K and $\pm 0.5\%$ RH, respectively. The relative humidity was varied in steps of $\Delta\text{RH} = 3\%$ between 2 and 98% at constant T (hydration dependent measurements). Alternatively, temperature dependent measurements were performed by changing T in steps of $\Delta T = 1$ K at constant RH = 50%.

The sample was allowed to equilibrate for 10 min in RH scans and for 2 min in temperature scans before measurement of the polarized IR spectra. No significant hysteresis effects between hydration and dehydration scans and between heating and cooling scans were detected confirming that the sample reached equilibrium in each measurement.

Results

Infrared active O–H stretching vibrations reveal molecular characteristics of lipid bound water

Water has a characteristic vibrational spectrum in the spectral range 3,000–3,800 cm^{-1} due the O–H stretches which is also present in the spectrum of hydrated lipids (see Fig. 1, and, e.g., Refs. Binder et al. 1998; Grdadolnik et al. 1994). This $\nu_{13}(\text{H}_2\text{O})$ band shows an

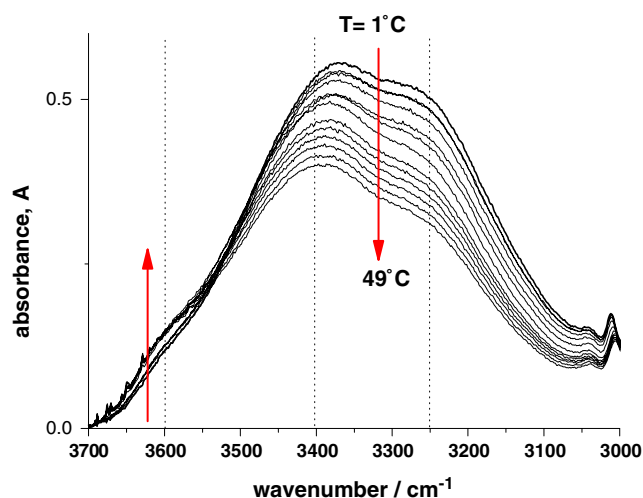


Fig. 1 Infrared absorbance spectra of the OH-stretching region of water adsorbed to POPC as a function of temperature. The arrows indicate the intensity decrease of the right-hand and the intensity increase of the left-hand bands which were assigned to network and multimer water, respectively. The lipid was hydrated at constant relative humidity, RH = 50%, which refers to about $R_{W/L} \approx 5$ water molecules bound per lipid (see Fig. 11 and Binder et al. 2001)

intensity maximum near $3,400\text{ cm}^{-1}$ with a marked low frequency shoulder near $3,250\text{ cm}^{-1}$ and a weaker high frequency shoulder near $3,600\text{ cm}^{-1}$.

An unambiguous interpretation of the $\nu_{13}(\text{H}_2\text{O})$ band is difficult because its shape and frequency can reflect (1) different energetic characteristics of adsorbed water molecules, (2) intra- and intermolecular couplings between the OH stretching vibrations within a particular water structure, and/or (3) Fermi resonance with 2ν the H–O–H bending mode (Bertie and Whalley 1964a, b; Walrafen 1967; Zundel 1969). Hence, the accurate determination of the stretching mode, depending on the degree of connectivity for each water molecule, is obviously impossible, but simple models have shown to be useful tools to estimate the extent of bonding of water molecules among each other and to polar surfaces.

We previously analyzed the OH-stretching region of water bound to different lipids (Binder 2003; Binder et al. 1997, 1998, 1999b, 2000; Binder and Pohle 2000; Binder and Zschörnig 2002) using such a relative simple interpretation proposed by Walrafen (1967) and Walrafen and Chu (1995) (see Ref. Binder et al. 1998 for a detailed discussion). It has been shown that the $\nu_{13}(\text{H}_2\text{O})$ band sensitively responds to the nature of intermolecular bonding and thus it is a suited probe of intermolecular water interactions.

Accordingly, the maximum near $3,400\text{ cm}^{-1}$ and the right-hand shoulder of the $\nu_{13}(\text{H}_2\text{O})$ near $3,250\text{ cm}^{-1}$

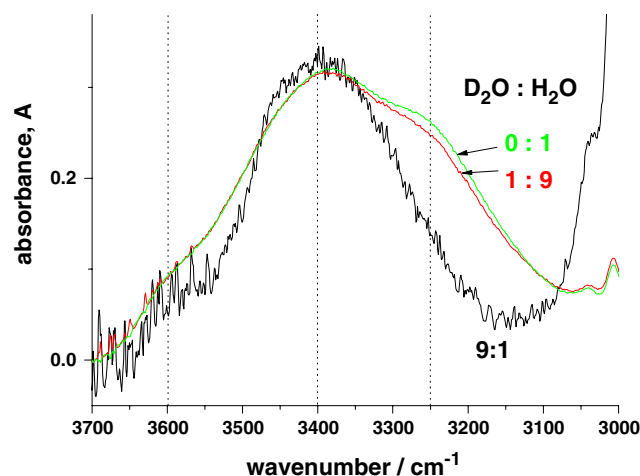


Fig. 2 Infrared spectra of the OH-stretching region of water bound to POPC. The lipid was hydrated at RH = 50% in an atmosphere of pure H_2O or in a mixed $\text{D}_2\text{O}:\text{H}_2\text{O}$ atmosphere of different composition. The addition of heavy water decouples the OH-stretches and thus isotopic dilution decreases the absorbance of bands due to the coupled OH vibrations of structured water

were attributed to O–H stretches of water molecules in an effective H-bonded structure (“network water”) whereas the weak high frequency shoulder near $3,600\text{ cm}^{-1}$ was assigned to water in a structure of disturbed hydrogen bonds (“multimer water”). Hence, both considered water types represent structured water, however of different connectivity with its surroundings: The network water is most likely involved in extended transient water networks forming up to four hydrogen bonds per water. The multimer water is ascribed to clusters of a few waters with about two or less H-bonds each.

The two IR-bands due to network water were assigned to symmetric ν_1 stretches where neighboring water molecules couple out of phase ($3,250\text{ cm}^{-1}$) and to a low-frequency mode which originates from a complex mixture of different vibrations with a major fraction of antisymmetric ν_3 stretches ($3,400\text{ cm}^{-1}$) (Bergren et al. 1978; McGraw et al. 1978). This interpretation is supported by hydration experiments in a mixed $\text{D}_2\text{O}:\text{H}_2\text{O}$ atmosphere (see Fig. 2). The relative absorbance of the right-hand shoulder near $3,250\text{ cm}^{-1}$ slightly decreases by addition of a small amount of D_2O (compare the spectra of pure water with that of the 1:9 mixture of $\text{D}_2\text{O}:\text{H}_2\text{O}$) and it almost completely disappears in the presence of an excess fraction of heavy water (see the spectrum of the 9:1 mixture). The trend confirms the assignment of this band to coupled O–H modes in a H-bonded structure because the increasing amount of O–D bonds pro-

gressively decouples the O–H stretches. An analogous assignment was performed on the basis of the IR linear dichroism of the $\nu_{13}(\text{H}_2\text{O})$ -band of water adsorbed onto PC headgroups (Binder 2003; Binder et al. 1998).

The integral absorbance over a spectral range of $\pm 20 \text{ cm}^{-1}$ about the selected position in the water spectrum, $A_i = \int A(\nu) d\nu / \Delta\nu$ ($I = 3,600$ or $3,250$), is directly related to the number of absorbing water molecules, n_i , if one uses a linear approximation and neglects band overlap and shifting, i.e., $A_i \propto \varepsilon_i \cdot n_i$. Here, ε_i is the molar extinction coefficient referring to the selected spectral range. For the absorbance ratio one consequently obtains $R_{3,600/3,250} = A_{3,600}/A_{3,250} \propto R_e \cdot R_{\text{II/I}}$ if one assumes that all lipid-bound water molecules per lipid are distributed between the considered two states, i.e., $R_{\text{W/L}} \propto n_{\text{I}} + n_{\text{II}}$ with $n_{\text{II}} \approx n_{3,600}$ and $n_{\text{I}} \approx n_{3,250}$ ($R_e = \varepsilon_{\text{II}}/\varepsilon_{\text{I}}$). The absorbance ratio is consequently directly related to the mole ratio $R_{\text{II/I}} = n_{\text{II}}/n_{\text{I}}$ which can serve as a rough measure of the mole ratio multimer-to-network water in the headgroup region of the lipids.

The maximum position of the main $\nu_{13}(\text{H}_2\text{O})$ band near $3,400 \text{ cm}^{-1}$ remains virtually unaffected by isotopic dilution (see Fig. 2 and Ref. Binder et al. 1999b). Consequently, this frequency is assumed to reflect the mean strength of water binding in the H-bonded network structure. A similar interpretation was previously proposed in a hydration study of polymeric collagen (Leikin et al. 1997). We calculated the center of gravity of the main $\nu_{13}(\text{H}_2\text{O})$ band, $\text{COG}_{3,400}$, as a robust estimate of its position.

The mole ratio water-to-lipid can be obtained from the ratio of the integral intensity of the $\nu_{13}(\text{H}_2\text{O})$ band, A_{W} , and of a suited internal standard which corrects A_{W} for dilution effects due to the swelling of the lipid film on the ATR surface. It was previously shown that the integral absorbance of the $\nu(\text{C}=\text{O})$ band of the lipid, $A_{\text{C}=\text{O}}$, near $1,730 \text{ cm}^{-1}$ provides a suited internal standard because it similarly responds on dilution as A_{W} (Binder et al. 2001). We therefore estimated the hydration degree of the lipid by means of $R_{\text{W/L}} = K_{\text{W}} \cdot A_{\text{W}}/A_{\text{C}=\text{O}}$, where the calibration factor K_{W} was obtained by comparison with gravimetric data (Binder et al. 2001).

The IR order parameter of an absorption band depends on the mean orientation of the absorbing transition moments with respect to the optical axis (see Materials and methods). The transition moment of the $\nu_{13}(\text{H}_2\text{O})$ -band near $3,250 \text{ cm}^{-1}$ was assigned to a symmetric ν_1 -mode. It roughly points along the bisector of the H–O–H bond angle. The respective order parameter, $S_{3,250}$, consequently characterizes the mean orientation of the water dipoles of structured water (see also Binder 2003; Binder et al. 1998).

Taking together, we are able to distinguish two types of water using the infrared spectrum of hydrated lipids in agreement with previous results (Walrafen 1967): The “network water” gives rise to the band centered at $3,250 \text{ cm}^{-1}$ which is associated with different modes of O–H vibrations in a regular hydrogen-bonded network while the “multimer water” causes the band near $3,600 \text{ cm}^{-1}$ due to vibrations of water in a structure with disturbed hydrogen bonds. The properties of the water can be characterized using several empirical parameters of the OH-stretching band: the absorbance ratio provides information about the relative population of both water types. The center of gravity of the main intensity component of the $\nu_{13}(\text{H}_2\text{O})$ band near $3,400 \text{ cm}^{-1}$ reflects the mean strength of water binding and the normalized integral absorbance of the $\nu_{13}(\text{H}_2\text{O})$ band provides the amount of water bound to the lipid, $R_{\text{W/L}}$. Finally, the mean orientation of structured water with respect to the membrane normal can be characterized using the infrared order parameter, $S_{3,250}$.

Temperature-dependent measurements

The intensity of the $\nu_{13}(\text{H}_2\text{O})$ band decreases with increasing temperature of a multibilayer POPC sample in an atmosphere of constant relative humidity (RH = 50%, see Fig. 1). Normalization with respect to dilution and calibration using gravimetric data shows that each lipid loses about one water upon heating over 50 K (see below, Fig. 11). Detailed inspection of the $\nu_{13}(\text{H}_2\text{O})$ band indicates that this trend is caused by the intensity decrease of the bands which were assigned to network water whereas the intensity band of the multimer water increases (see the arrows in Fig. 1). These opposite intensity changes give rise to an isobestic point near $3,450 \text{ cm}^{-1}$, which provides a strong argument in favor of an equilibrium of two water types (Walrafen 1967; Walrafen and Chu 1995).

To quantify the observed intensity changes we plotted the absorbance ratio of the left-hand and right-hand shoulders, $R_{3,600/3,250}$, as a function of temperature (see Fig. 3). It linearly increases in the range of the gel phase below 19°C and in the range of the liquid-crystalline phase above 24°C . The step-like break in the course of $R_{3,600/3,250}$ reflects the gel-to-liquid crystalline melting transition of the lipid. The positive slope of $R_{3,600/3,250}$ with temperature gives clear evidence that heating increases the fraction of multimer water in the hydration shell of the lipids.

For a more detailed evaluation we calculated the difference spectra of subsequent temperature points,

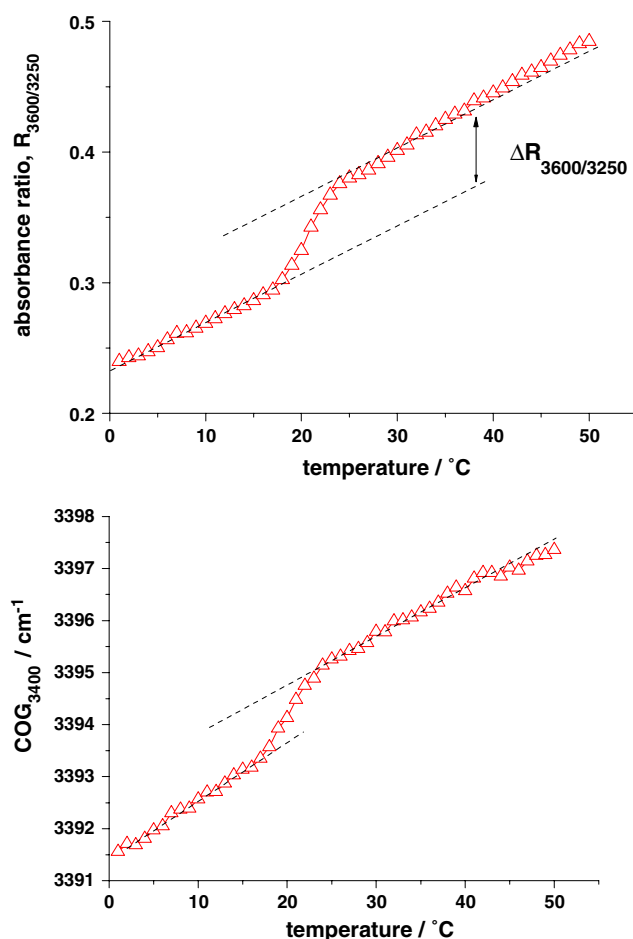


Fig. 3 Absorbance ratio of the $\nu_{13}(\text{OH})$ subbands at 3,600 and 3,250 cm^{-1} (part *above*) and the center of gravity of the main intensity component near 3,400 cm^{-1} as a function of temperature at RH = 50%. $R_{3,600/3,250}$ estimates the relation between the amount of multimer and structured water bound to POPC. The $\text{COG}_{3,400}$ (inversely) correlates with the mean binding energy of network water (see text). The stepwise increase of both parameters is caused by the gel-to-liquid crystalline phase transition of the lipid. The respective increment $\Delta R_{3,600/3,250}$ is essentially identical with that observed upon heating over 15–20 K in the pure phase ranges

$\Delta A(T) = A(T) - A(T - \Delta T)$ with $\Delta T = 2$ K (see Fig. 4). These difference spectra typically show a marked (negative) minimum in the spectral region of the network water and a very weak (positive) maximum for the multimer water in the pure phase ranges of the lipid (see, e.g., $T = 17^\circ\text{C}$ for the gel, and 25°C for the liquid-crystalline phase in Fig. 4). This result indicates that heating is mainly paralleled by the removal of network water from the lipid headgroups. In the vicinity of the main phase transition of the lipid the weak maximum of $\Delta A(T)$ near 3,600 cm^{-1} considerably grows in intensity (see $T = 19, 21$ and 23°C in Fig. 4).

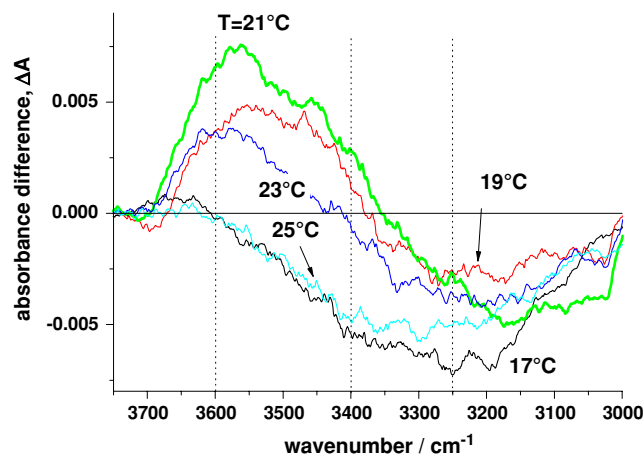


Fig. 4 Difference spectra, $\Delta A(T) = A(T) - A(T - \Delta T)$ with $\Delta T = 2^\circ$, of the OH-stretching region of water bound to POPC at RH = 50%. The respective absorbance spectra are shown in Fig. 1. The negative and positive regions of $\Delta A(T)$ indicate that network water transforms into multimer water upon heating

Hence, lipid melting gives rise to the transfer of water from the network state into the multimeric state in considerable amounts. In addition, the membrane slightly imbibes water at the gel-to-liquid crystalline phase transition (Binder et al. 1999b; Faure et al. 1997). The spectral data show that this incremental water predominantly adsorbs as multimer water.

The center of gravity of the main $\nu_{13}(\text{H}_2\text{O})$ band shifts towards smaller wavenumbers upon heating. This change reflects the gradual weakening of water structure according to our interpretation (Fig. 3).

The temperature scans were repeated for different values of the relative humidity, RH = const. The obtained absorbance ratio, $R_{3,600/3,250}$, shows a similar behavior in all cases (Fig. 5). The phase transition temperature, however, decreases with increasing RH as indicated by the respective shift of inflection point in the courses of $R_{3,600/3,250}$. The shift of the phase transition can be rationalized in terms of the hydration pressure acting on the lipid. It decreases with increasing RH and this way the phase transition temperature decreases in analogy with the effect of a decreasing external hydrostatic pressure (Binder 2003; Pfeiffer et al. 2003a, b).

The lower part of Fig. 5 shows the infrared order parameter, $S_{3,250}$, of the right-hand shoulder of the $\nu_{13}(\text{H}_2\text{O})$ band. It provides a measure of the mean orientation of the water dipoles relative to the membrane normal. The drop of $S_{3,250}$ at the phase transition shows that the melting of the lipids is accompanied by the partial disordering of the water dipoles and/or by their concerted reorientation from a more parallel

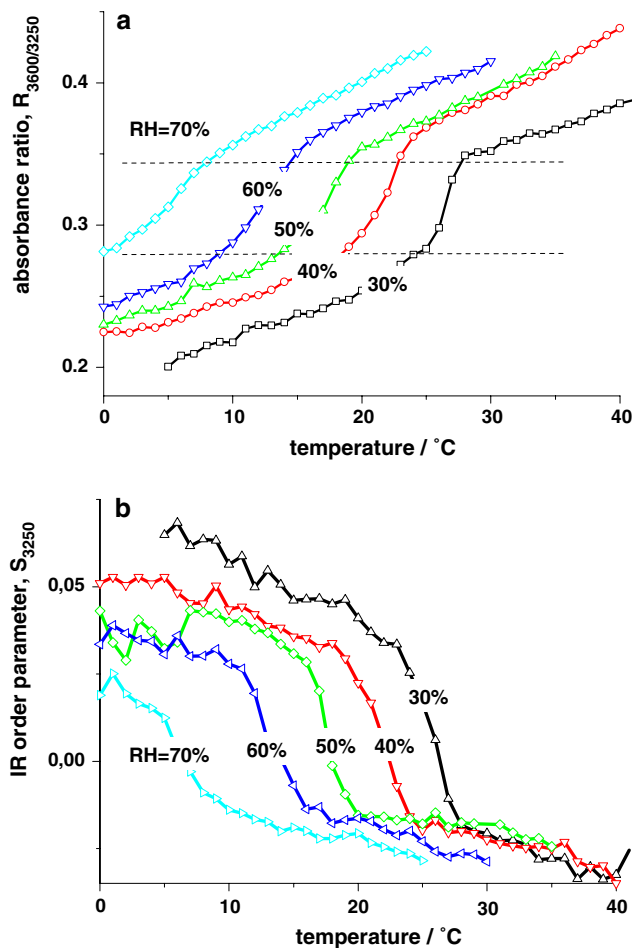


Fig. 5 Temperature dependent changes of the absorbance ratio $R_{3,600/3,250}$ (a) and of the IR order parameter, $S_{3,250}$ (b) of water bound to POPC. The sample was hydrated in an atmosphere of constant relative humidity referring to a water-to-lipid mole ratio of $R_{W/L} \approx 3$ (RH = 30%), 4 (40%), 5 (50%), 6 (60%), and 6.5 (70%) at $T = 25^\circ\text{C}$. The phase transition temperature decreases with increasing hydration. Note that the increment $\Delta R_{3,600/3,250}$ at the phase transition remains virtually constant as indicated by the two horizontal lines

towards a more perpendicular orientation relative to the membrane normal.

Hydration-dependent measurements

In a second line of experiments we varied the relative humidity in the ambient atmosphere of the lipid film at constant temperature. The increase of the intensity of the $\nu_{13}(\text{H}_2\text{O})$ band with increasing RH reflects the progressive sorption of water (see Fig. 6). The scaled integral absorbance of the $\nu_{13}(\text{H}_2\text{O})$ band provides the adsorption isotherm as described above (see Fig. 11). It shows that the total number of water molecules per lipid continuously increases from $R_{W/L} \approx 0.5$ to >12 upon increasing RH from 2 to 98%. The slope of the

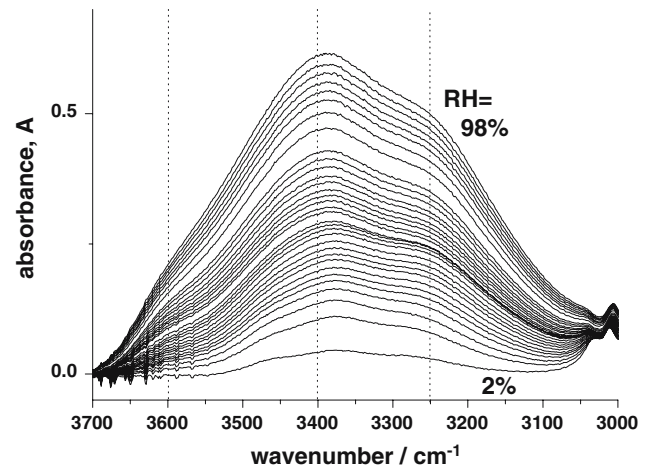


Fig. 6 Infrared absorbance spectra of the OH-stretching region of water adsorbed to POPC as a function of relative humidity at $T = 25^\circ\text{C}$. The RH-increment of two subsequent spectra is $\Delta\text{RH} = 3\%$ which refers to an increment of the number of adsorbed water per lipid of $\Delta R_{W/L} = 0.3\text{--}0.6$

isotherm is nearly a constant, $dR_{W/L}/d\text{RH} \approx 0.09$, in the range 10–80% but it nearly doubles for $\text{RH} > 80\%$ ($dR_{W/L}/d\text{RH} \approx 0.15$). As a rule of thumb, the change of RH by 10% changes the number of water per lipid by about one at $\text{RH} < 80\%$. This result is in agreement with recent studies which report a linear regime of water sorption at $\text{RH} < 90\%$ which is followed by an exponential regime at $\text{RH} > 90\%$ (Caracciolo et al. 2005). Presumably our humidity-titration technique underestimates the hydration degree in the latter range, especially for $\text{RH} > 95\%$. Note that small errors in the adjustment of RH in exponential regime cause large effects in the amount of sorbed water especially at humidities near 100%.

The plot of the absorbance ratio of the left-hand and right-hand shoulders of the $\nu_{13}(\text{H}_2\text{O})$ band, $R_{3,600/3,250}$, as a function of RH shows a similar course as the respective plot of $R_{3,600/3,250}$ as a function of the temperature (compare Figs. 7 and 3). The step between the two linear ranges is caused by the lyotropic, i.e. hydration-induced gel-to-liquid crystalline phase transition of the lipid. The positive slope of $R_{3,600/3,250}$ indicates that the accumulation of water in the head-group region of the lipids is accompanied by the increase of the fraction of multimer water in analogy with the temperature-induced changes of $R_{3,600/3,250}$ discussed above.

To get further insights into the details of the water arrangement we calculated the difference spectra between subsequent RH-values, $\Delta A(\text{RH}) = A(\text{RH}) - A(\text{RH} - \Delta\text{RH})$ with $\Delta\text{RH} = 3\%$ (Fig. 8). The difference spectrum $\Delta A(\text{RH})$ is exclusively positive in contrast to $\Delta A(T)$ (compare Figs. 8 and 4). This result shows

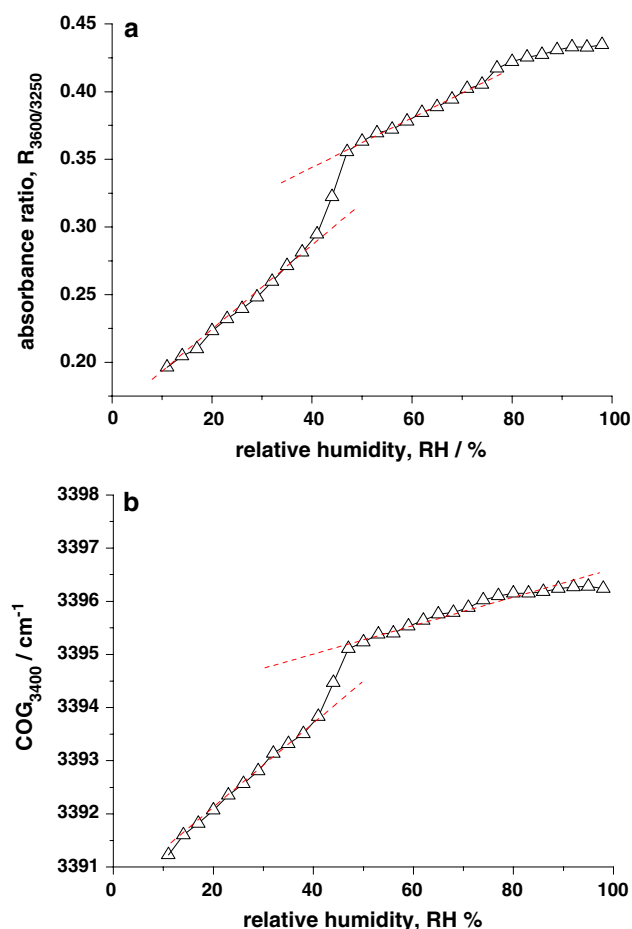


Fig. 7 Absorbance ratio of the $\nu_{13}(\text{OH})$ subbands at 3,600 and 3,250 cm^{-1} (part above) and the center of gravity of the main intensity component near 3,400 cm^{-1} as a function of the relative humidity at $T = 25^\circ\text{C}$. The stepwise increase of both parameters is caused by the lyotropic gel-to-liquid crystalline phase transition of the lipid

that water referring to all considered spectral regions adsorbs to the lipid upon increasing RH. Each hydration step induces, on the average, the binding of $\Delta R_{\text{W/L}} \approx 0.3\text{--}0.6$ water molecules per lipid (see above and Fig. 11).

The shape of the difference spectra reports about subtle changes in the arrangement of the water in the polar region of the membrane which were induced by the change of the water activity in the system. The right-hand shoulder due to structured water is maximum at small hydration degrees (see Fig. 9, $\text{RH} = 14\%$). This effect reflects the fact that the water initially incorporates into a highly ordered water structure of the primary hydration shell.

The most pronounced spectral effect on the difference spectra takes place at the lyotropic phase transition near $\text{RH} = 44\%$ (see Figs. 8, 9). The right-hand shoulder at 3,250 cm^{-1} nearly completely vanishes

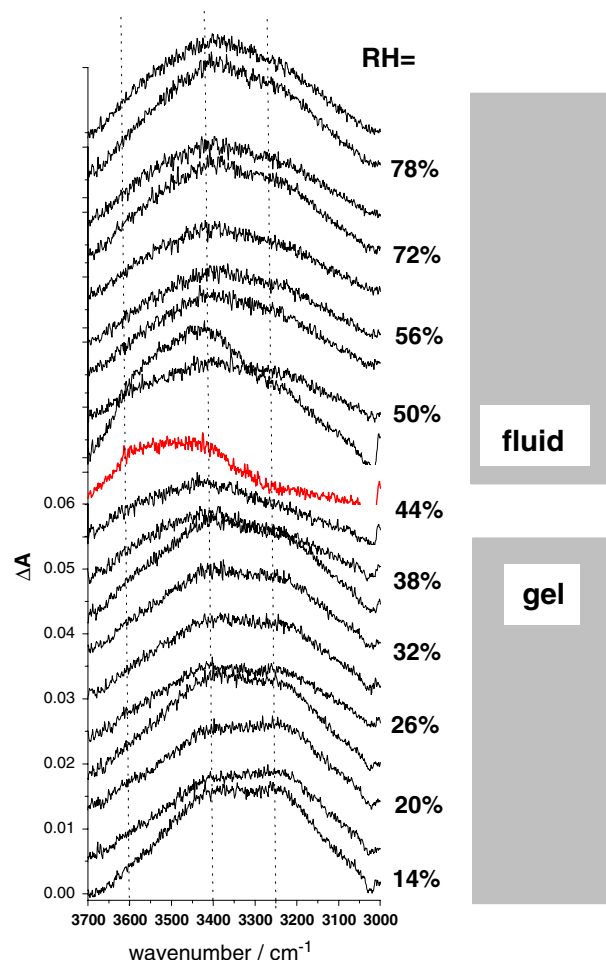


Fig. 8 Difference spectra, $\Delta A(\text{RH}) = A(\text{RH}) - A(\text{RH} - \Delta \text{RH})$ with $\Delta \text{RH} = 3\%$, of the OH-stretching region of water bound to POPC at $T = 25^\circ\text{C}$. The respective absorbance spectra are shown in Fig. 6. The right part indicates the phase state of the lipid. Note the changing shape of $\Delta A(\text{RH})$ especially at the phase transition (see also Fig. 9)

whereas the intensity of the left-hand band near 3,600 cm^{-1} considerably increases. This particular shape of $\Delta A(\text{RH} = 44\%)$ can be understood if the water sorbs nearly exclusively as multimer water in analogy with the change of water structure at the thermotropic phase transition at which network water transfers into multimer water. Hence both, thermotropic and lyotropic measurements clearly indicate that the liquid-crystalline phase adsorbs a significant larger fraction of multimer water than the gel state. The upwards shift of the center of gravity of the main $\nu_{13}(\text{H}_2\text{O})$ band with RH indicates the weakening of the mean strength of water binding upon progressive hydration (Fig. 7b).

We repeated the hydration experiment at different temperatures. The plots of the spectral ratio $R_{3,600/3,250}$ resemble each other independent of T (see Fig. 10a).

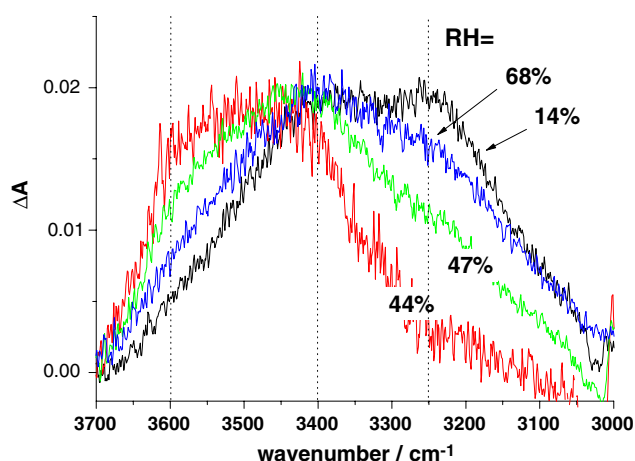


Fig. 9 Difference spectra, $\Delta A(RH)$, for selected values of the relative humidity. The difference spectra were normalized with respect to the maximum intensity. Note the different intensity of the left- and right-hand component bands referring to the sorption of multimer and of network water, respectively. The shape of $\Delta A(RH = 44\%)$ can be explained by the transformation of network water into multimer water at the phase transition

Heating shifts the phase transition towards smaller hydration degrees. The IR order parameter $S_{3,250}$ indicates that the water dipoles reorient upon hydration in an analogous fashion as upon heating (Fig. 10b).

Discussion

We studied the hydration of lipid membranes using two series of experiments by varying either the temperature or the relative humidity. The properties of water in the hydration layer of the lipids were characterized using different spectral parameters of the $\nu_{13}(H_2O)$ band: its mean position, $COG_{3,400}$; the intensity ratio of its high and low frequency shoulders $R_{3,600/3,250}$; and the IR order parameter, $S_{3,250}$. The considered spectral parameter change in a very similar fashion in both experimental series with increasing T and RH , respectively, indicating the continuous increase of the fraction of less-structured multimer water, the decrease of the mean binding strength in the network of H-bonds, the disordering of the orientation of the water dipoles and/or their reorientation from a more parallel towards a more perpendicular orientation with respect to the membrane normal. The lipid exists in the gel phase at small T and RH and transforms into the liquid crystalline phase upon heating and/or hydration. The phase transition is accompanied by a stepwise change of the parameters studied.

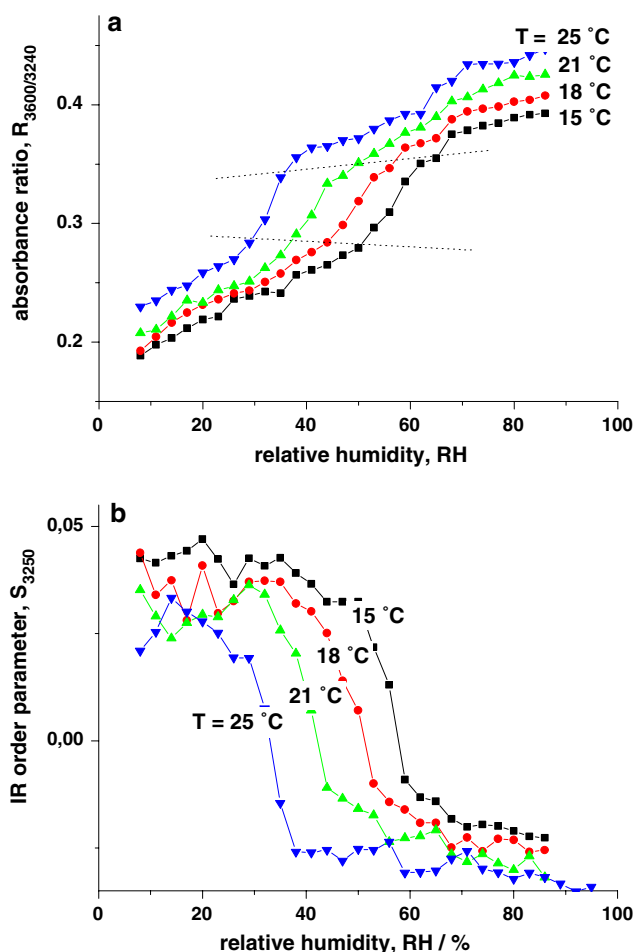


Fig. 10 Hydration dependent changes of the absorbance ratio $R_{3,600/3,250}$ (a) and of the IR order parameter, $S_{3,250}$ (b) of water bound to POPC which was hydrated at constant temperature. The hydration degree at the phase transition decreases with increasing temperature. Note that the increment $\Delta R_{3,600/3,250}$ at the phase transition remains virtually constant as indicated by the two horizontal lines

The estimation of the energetic cost of water removal using spectral data is difficult. Figure 12 re-plots the center of gravity and the intensity ratio $R_{3,600/3,250}$, obtained in both series of experiments (see also Figs. 3, 7) as a function of the mole ratio water-to-lipid, $R_{W/L}$ (Fig. 11). It turns out that the magnitude of change in the spectral parameters upon gradually removing the water from the lipid from the state of full hydration to the nearly anhydrous state is approximately the same as that from cooling hydrated lipid by 40–50 K. Note that both, the lyotropic and the thermotropic changes include the phase transition of the lipid with nearly identical increments of the absorbance ratio $\Delta R_{3,600/3,250} \approx 0.05$.

Making use of the specific heat of water ($C_p \approx 75$ J/mol K) and ice Ih (38 J/mol K; Murphy and Koop

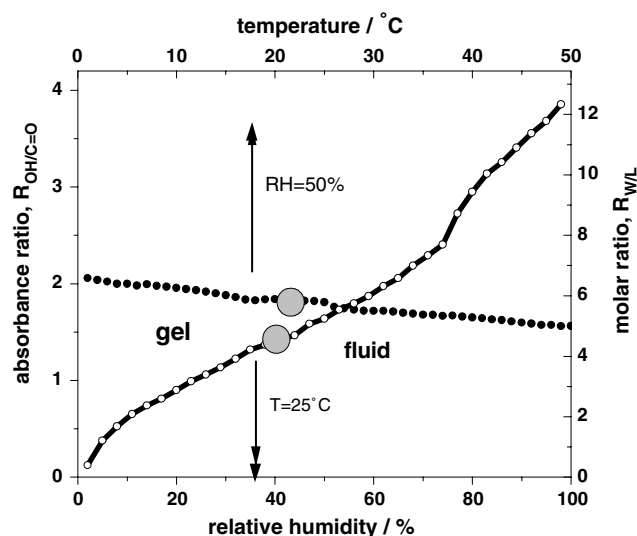


Fig. 11 Normalized integral absorbance of the $\nu_{13}(\text{OH})$ band of water bound to POPC as a function of the relative humidity at $T = 25^\circ\text{C}$ (axis below) and as a function of temperature at $\text{RH} = 50\%$ (axis above). The integral absorbance of the $\nu_{13}(\text{OH})$ band was normalized using the integral absorbance of the $\text{C}=\text{O}$ stretching band near $1,730\text{ cm}^{-1}$ to get a measure of the number of water molecules per lipid, $R_{\text{W/L}}$ (see right axis). For calibration we used gravimetric data (see Ref. Binder et al. 2001 for details). The gray dots indicate the gel-to-liquid crystalline phase transition

2005) as a upper and lower limit for that of lipid-bound water one can estimate that the enthalpy cost of the rearrangement is of the order of 2–4 kJ/mol of water. This value amounts to about 10–20% of the total Gibbs free energy of dehydration of the lipid (15–20 kJ/mol; Binder et al. 1999b, 2001) and to about 5–10% of the heat of evaporation of bulk water (~45 kJ/mol). The former value quantifies the work per mole of lipid which should be applied to remove the water from the lipid bilayer whereas the latter value characterizes the enthalpy per mole of water which is stored in the interactions with neighboring water molecules. Note that the magnitude of the change of the spectral parameters at the melting transition of the lipid is roughly the same as that observed upon heating from 1 to 15°C . Consequently about 30% of the estimated energetic costs refer to the rearrangement of water structure due to the melting of the lipid. Despite of its approximative character, this estimation demonstrates the energetic significance of water hydrogen bond rearrangement due to the lipid headgroups. Probably it even underestimates the real costs because the strength of the water-headgroup H-bonds exceeds that of the water–water bonds.

The mean band position $\text{COG}_{3,400}$ and the ratio $R_{3,600/3,250}$ change smoothly with the water content,

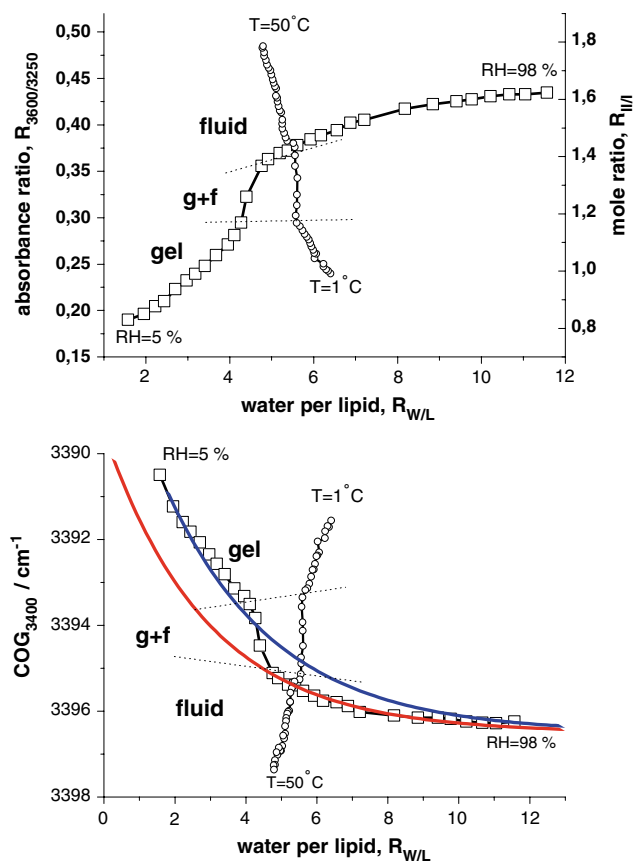


Fig. 12 Absorbance ratio of the $\nu_{13}(\text{OH})$ subbands at 3,600 and $3,250\text{ cm}^{-1}$ (part above) and the center of gravity of the main intensity component near $3,400\text{ cm}^{-1}$ (part below) as a function of the mole ratio water to lipid. The data were obtained from the temperature ($\text{RH} = 50\%$, small symbols) and humidity ($T = 25^\circ\text{C}$, large symbols) scans described above. The two exponentially decaying curves in the part below were calculated with the parameters $(\Delta\text{COG}, R_0) = (7\text{ cm}^{-1}, 2.9)$ and $(10\text{ cm}^{-1}, 3.1)$ for the fluid and the gel phase, respectively, and $\text{COG}_\infty = 3,396.5\text{ cm}^{-1}$ (see text)

$R_{\text{W/L}}$, reflecting the continuous rearrangement in the H-bond network of structured water and the continuous increase of the fraction of multimer water. The energetic characteristics can be approximated by an exponential decay law of the form, $\text{COG}_{3,400}(R_{\text{W/L}}) \approx \Delta\text{COG} \cdot \exp(-R_{\text{W/L}}/R_0) + \text{COG}_\infty$, with a decay constant of $R_0 \approx 2.9$ (fluid)– 3.1 (gel) (see the curves in Fig. 12). The initial values ΔCOG of the two calculated decays are shifted in vertical direction by 3 cm^{-1} each to another to fit the experimental data for each phase separately and this way to account for the step at the gel to liquid crystalline phase transition. The results show that the change of the phase state only weakly affects the decay constant, and thus the number of water molecules which are affected by the surface.

The spatially varying perturbation of water has been considered as the possible source of the exponential

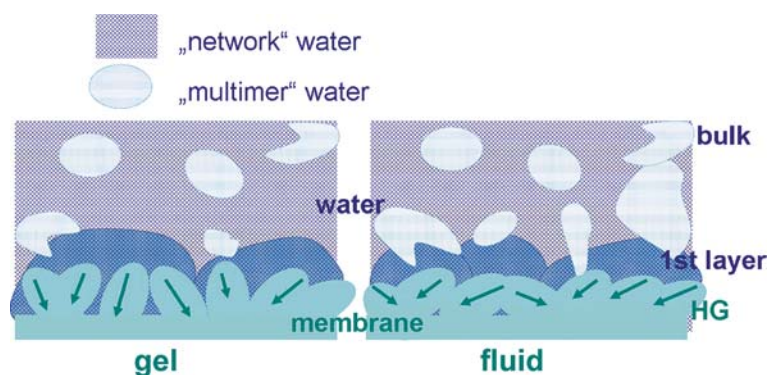


Fig. 13 Schematic cartoon of the polar interphase of POPC bilayers in the gel and fluid phases. The water forms transient microdomains of two possible states: low density “network” water of high connectivity and higher density “multimer” water of lower connectivity. The amount of multimer water increases with increasing distance from the lipid headgroups (HG) and upon transformation of the lipid from the gel into the fluid phase.

The primary hydration layer of network water (1st layer) forms relative strong H-bonds with the phosphate and carbonyl groups of the lipid. The headgroup N^+-P^- dipoles point on the average more parallel to the membrane surface in the fluid phase (see arrows). The water dipoles in the 1st layer tend to orient antiparallel with respect to the headgroup dipoles (see text). The size and shape of the microdomains are hypothetical

hydration force measured between membranes upon mutual approach to interbilayer distances smaller than a few nanometers (Le Neveu et al. 1976; Leikin and Parsegian 1993; Parsegian et al. 1979; Rand and Parsegian 1989). Note that also the free energy of hydration follows an exponential decay law with a decay constant of $R_0 \approx 2.7$ (Binder et al. 1999a). The agreement with the decay characteristics of the spectral parameter $COG_{3,400}$ confirms its interpretation as a measure of the stability of the network of H-bonds. It also supports a solvation-based model of hydration forces.

Computer simulations have shown that the strength of the hydrogen bonds formed by the water near lipid membranes decreases with changing interaction partner in the following order: water–phosphate group > water–O–CO (sn1) > water–O–CO (sn2) > water–water (Bhide and Berkowitz 2005; Klose et al. 1985). That means that any H-bond between the water and the lipid is stronger than the H-bonds between water molecules. The mean number of the strong H-bonds formed between the water and the lipid increases upon decreasing distance of the water from the bilayer, particularly, from zero for the water in the second hydration layer to about two bonds for water which resides in the bilayer near the carbonyl groups. Hence, the change of the spectroscopic parameter $COG_{3,400}$ in the hydration experiment presumably reflects the relative increase of the amount of strong water–headgroup interactions with decreasing hydration degree.

The OH-stretching band has been conceivably interpreted by a simplified two-state model, which discriminates network and multimer water. Both water types are assumed to reflect H-bond structures of dif-

ferent connectivity. Note that even at low hydration degrees of the studied lipid the $\nu_{13}(H_2O)$ band maintains its basic shape observed in bulk water and at high hydration degrees as well. The increasing number of contacts of the water with the lipid headgroups obviously disturbs but not completely rearranges the basic H-bonding structure. In other words, the spectral data reflect the fact that the water effectively fits around the polar moieties of the lipid forming a local H-bonding network which is similar to that in pure water despite the fact that it includes the phosphate and carbonyl groups and neighboring waters as well. The amount of weakly connected multimer water decreases but it still exists at small hydration degrees. This fact reflects the transient character of the H-bonded structures where network water transforms into multimer water and vice versa on a timescale exceeding that of the molecular vibrations which define the time resolution of the method. As a consequence IR spectroscopy essentially sees the ensemble average of both structures.

The $\nu_{13}(H_2O)$ band of pure water changes upon heating in a very similar fashion as the $\nu_{13}(H_2O)$ band of lipid bound water reported here (see Walrafen 1967; Walrafen and Chu 1995 for comparison). This similarity confirms our conclusion that the equilibrium between the two considered water types with transient transformations in both directions is obviously a common property of both, bulk and interfacial water.

From independent studies on the properties of pure water it became evident that this liquid is composed of dynamically transforming microdomains of two very different binding types (Kamb 1968; Vadamuthu et al. 1994): the first one of type I is the highly ordered

tetrahedral water–water bonding which forms water clusters similar to that in ordinary ice Ih. The second type II is a non-regular tetrahedral bonding similar to that in Ice IIh. Consequently, liquid water can be considered as a two-state mixture of both water types (Vedamuthu et al. 1994). Type I water is of lower density than type II water. Upon heating from 0 to 50°C the fraction of low-density water decreases from $x_I \approx 0.4$ –0.3 whereas, the density of both water types remains virtually unchanged. Consequently, the predominant effect of temperature on liquid water is the change of the fraction of water types with consequences for the total density of water.

The similar spectral changes of bulk and of lipid-bound water upon heating at one-hand side and of lipid-bound water upon heating and upon hydration on the other hand side suggest an analogous structural origin. Following this idea, the water in the hydration layer of the lipid bilayer is arranged in dynamically transforming microdomains of well-structured, low-density network water of type I and of less-structured dense multimer water of type II (see Fig. 13 for illustration). The polar moieties of the lipid gradually affect the water structure and thus also the equilibrium between both water types giving rise to the perturbation of water arrangement compared with that of the bulk state. According to our spectroscopic data they exert a structuring effect on the water molecules in their first hydration shell which forms H-bonds with the oxygen of the phosphate and carbonyl groups. As a consequence, the fraction of low-density network water is increased in the primary hydration shell compared with that in bulk water. Recent molecular dynamics studies indicate that the density of water continuously decreases the closer the water residues to the lipid bilayer in agreement with our result (Aman et al. 2003; Bhide and Berkowitz 2005). It should, however, taken into account that this trend is, at least partly, caused by the “dilution” of the water by the lipid headgroups and not necessarily by the loosening of water packing in the more tetrahedral arrangement of type I.

The spectroscopic ratio, $R_{3,600/3,250}$, is directly related to the mole ratio of both water types, i.e., $R_{3,600/3,250} \propto R_{II/I} = R_{\text{mult}/\text{net}}$ (see above) which is, however, scaled by the ratio of the respective integral molar extinction coefficients, R_ϵ . Let us assume for a rough estimation that R_ϵ is independent of hydration and temperature. Then extrapolation of $R_{3,600/3,250}$ to full hydration and making use of the data for the temperature dependence of the fraction of both water types in bulk water (Vedamuthu et al. 1994) provides an estimate of $R_{II/I}$ for the water in the polar interface of the bilayer (see right axis in Fig. 12). Accordingly, the ratio

$R_{II/I}$ roughly halves upon dehydration from $R_{II/I} \approx 1.6$ at full hydration to $R_{II/I} \approx 0.8$ at $R_{W/L} < 2$. This change of the mole ratio $R_{II/I}$ refers to the increase of the fraction of network water from $x_I \approx 0.3$ –0.6. The latter value equals that of supercooled water at -25°C .

Details of the H-bonding network of water near phospholipid were studied using computer simulation (Bhide and Berkowitz 2005). The progressive approach of the water to the bilayer is mainly paralleled by two effects: (1) the most probable total number of hydrogen bonds per water progressively reduces from about 3.7 in bulk water to about 3.1 for water which is buried in the membrane near the carbonyl groups; and (2) the stronger water-headgroup H-bonds partly replace the water–water hydrogen bonds. Accordingly, the network water near the membrane is characterized by less but stronger H-bonds per water, a prediction that agrees with our spectroscopic results.

The perturbation of water structure in the polar interface of the membrane is clearly modulated by the phase state of the lipid. The highly ordered gel phase gives rise to relatively high fraction of structured network water compared with the liquid crystalline phase. About one third of the total hydration induced change of the fraction of network water should be attributed to the melting transition. In other words, the disordering of the lipid also disturbs the arrangement of water. This change is associated with enthalpic costs of about 0.5–1 kJ/mol which amount to about one third of the total costs according to our estimation (see above).

The considered IR order parameter roughly reflects the mean orientation of the water dipoles with respect to the membrane normal. Essentially two limiting, virtually undistinguishable situations can cause the decrease of the order parameter $S_{3,250}$ observed with progressive hydration and/or upon heating, namely the disordering of the orientation of the water dipoles, i.e. the loss of correlation between their mutual orientations and/or their concerted, than means, correlated reorientation from a more parallel towards a more perpendicular orientation with respect to the membrane normal. Note that the bilayer expands laterally upon heating and/or hydration (Binder and Gawrisch 2001). This trend is accompanied by the reorientation of the dipole of the zwitterionic lipid headgroup which, on the average, tends to incline away from the membrane normal with increasing lateral area per lipid in the bilayer and by the disordering of their orientation due to an increased mobility in the fluid phase. The ordering and mean orientation of the water dipoles obviously follow the same tendencies as the headgroup dipoles which point along the interconnecting line between the charged nitrogen and phosphate atoms of

the phosphatidylcholine moiety. This conclusion is supported by the fact that the water order parameter similarly changes as selected IR order parameters of the phosphate group whereas the order parameter of the C=O group as an alternative hydration site shows different properties (Binder 2003). The correlation between water and headgroup orientation suggests that both dipoles orient antiparallel on the average. Indeed, computer studies have shown that water builds highly structured regions in the vicinity of phospholipid headgroups that tend to compensate the headgroup dipole moment (Alper et al. 1993; Binder and Peinel 1985; Klose et al. 1985; Peinel et al. 1983a; Yegiazaryan et al. 2006; Zhou and Schulten 1995).

Hence, the water macroscopically orients relatively to the membrane owing to the dipolar interactions between the water and the headgroup dipoles and because of the H-bonding between water hydrogen and the oxygen of the carbonyl and especially the phosphate groups of the lipid. The cooperative orientation of the water in the vicinity of the lipid headgroups was previously used as the criterion to identify lipid-bound “perturbed” water which is characterized by a non-zero order parameter (Aman et al. 2003). This study reports that about six waters located nearest to the headgroup possess a positive and the next 10–11 water a negative order parameter, with predominantly (anti-)parallel and perpendicular orientation with respect to the membrane normal, respectively. Already first computer simulations on water near a layer of lipid headgroups revealed that the perturbed, interfacial water arranges in parallel layers (Binder and Peinel 1985; Klose et al. 1985). The first layer comprises about 4–5 water molecules directly attached with the lipid via H-bonds. The “next” 6–7 water in the second layer are completely coordinated by water molecules. This result is in agreement with NMR quadrupole splitting measurements on heavy water which also suggested the occurrence of two hydration shells with about 5 and 6–7 water per lipid, respectively (Arnold et al. 1981, 1983).

The IR-spectroscopic data reflect a rather continuous change of the water properties with increasing distance from the membrane. Network and multimer water distribute across the whole polar interface with changing composition and orientation. The assumption of a single “primary” hydration layer and bulk-like properties of the water beyond this primary layer thus appeared as an oversimplification. On the other hand, our results show that the water in the hydration shell possesses similar H-bonding characteristics compared with bulk water even in the primary hydration shell. It seems that the question is not about the relevance of one, two or even more hydration layers but about the

thickness of the interphase, i.e. the range of the structuring effect that exert the headgroups on the water. The interphase includes at least water from the second hydration layer for decay constants of 2.5–3.0 waters per lipid. The properties of the interphase also depend on the mobility and orientation of the lipid headgroups which gradually change at the gel-to-liquid crystalline phase transition. Note that crystalline phases of lipids with immobilized PC-headgroups give rise to drastic changes of both the water and headgroup properties which, for example, cause the drastic drop of the decay constant (Binder et al. 1998).

Conclusions

The perturbation of interfacial water near phospholipid membranes becomes manifest in its orientation, H-bonding and energetic characteristics. Infrared spectroscopy of the O–H stretching region allows the characterization of these properties of bound water in terms of empirical parameters with relatively high resolution. Hydration/dehydration studies with varying water content provide insights into the water arrangement in different regions of the hydration shell of the membrane. The interpretation of such data must take into account the fact that the properties of the whole system and thus also that of the lipid are a function of the water content. Dehydration of POPC induces the phase transformation from the liquid crystalline into the gel phase where the changes in the water and lipid properties are interrelated. The IR perspective adds new facets about the existing picture of the hydration shell of lipid bilayers. Particularly, it enables the detailed characterization of the H-bonding of water and its perturbation due to the presence of the polar interface. Spectrally the water can be split into two fractions, network and multimer water, where the amount of network water decreases with temperature and hydration. The network water is characterized by stronger H-bonds and a higher ordering.

In perspective the analogous spectral analysis for other lipid systems is expected to reveal subtle differences in the properties of sorbed water with consequences for the properties of the polar interphase of lipid membranes.

References

- Alper HE, Bassolino-Klimas D, Stouch TR (1993) The limiting behaviour of water hydrating a phospholipid monolayer. A computer simulation study. *J Phys Chem* 99:5547–5559

- Aman K, Edholm O, Hakanson P, Westlund P-O (2003) Structure and dynamics of interfacial water in an α phase lipid bilayer from molecular dynamics simulations. *Biophys J* 85:102–115
- Arnold K, Pratsch L, Gawrisch K (1983) Effect of poly(ethylene glycol) on phospholipid hydration and polarity of the external phase. *Biochim Biophys Acta* 728:121–128
- Arnold K, Löbel E, Volke F, Gawrisch K (1981) ^{31}P -NMR investigations of phospholipids. *Stud Biophys* 82:207–214
- Arrondo JLR, Goni FM, Macarulla JM (1984) Infrared spectroscopy of phosphatidylcholines in aqueous suspensions. A study of the phosphate group vibrations. *Biochim Biophys Acta* 794:165–168
- Bergren MS, Schuh D, Sceats MG, Rice SA (1978) The OH-stretching region infrared spectra of low density amorphous solid water and polycrystalline ice Ih. *J Chem Phys* 69:3477–3482
- Bertie JE, Whalley E (1964a) Infrared spectra of ices Ih and Ic in the range 4000 to 350 cm^{-1} . *J Chem Phys* 40:1637–1645
- Bertie JE, Whalley E (1964b) Infrared spectra of ices II, III, and V in the range 4000–350 cm^{-1} . *J Chem Phys* 40:1646–1659
- Bhide SY, Berkowitz ML (2005) Structure and dynamics of water at the interface with phospholipid bilayers. *J Chem Phys* 123:224702
- Binder H (2003) The molecular architecture of lipid membranes—new insights from hydration-tuning infrared linear dichroism spectroscopy. *Appl Spectrosc Rev* 38:15–69
- Binder H, Gawrisch K (2001) Effect of unsaturated lipid chains on dimensions, molecular order and hydration of membranes. *J Phys Chem B* 105:12378–12390
- Binder H, Peinel G (1985) Behaviour of water at membrane surfaces—a molecular dynamics study. *J Mol Struct* 123:155–163
- Binder H, Pohle W (2000) Structural aspects of lyotropic solvation-induced transitions in phosphatidylcholine and phosphatidylethanolamine assemblies revealed by infrared spectroscopy. *J Phys Chem B* 104:12039–12048
- Binder H, Schmiedel H (1999) Infrared dichroism investigations on the acyl chain ordering in lamellar structures I. The formalism and its application to polycrystalline stearic acid. *Vib Spectrosc* 21:51–73
- Binder H, Zschörnig O (2002) The effect of metal cations on the phase behavior and hydration characteristics of phospholipid membranes. *Chem Phys Lipids* 115:39–61
- Binder H, Anikin A, Kohlstrunk B, Klose G (1997) Hydration induced gel states of the dienic lipid 1,2-bis(2,4-octadecanoyl)-sn-glycero-3-phosphorylcholine and their characterization using infrared spectroscopy. *J Phys Chem B* 101:6618–6628
- Binder H, Gutberlet T, Anikin A, Klose G (1998) Hydration of the dienic lipid dioctadecadienoylphosphatidylcholine in the lamellar phase—an infrared linear dichroism and X-ray study on headgroup orientation, water ordering and bilayer dimensions. *Biophys J* 74:1908–1923
- Binder H, Kohlstrunk B, Heerklotz HH (1999a) A humidity titration calorimetry technique to study the thermodynamics of hydration. *Chem Phys Lett* 304:329–335
- Binder H, Kohlstrunk B, Heerklotz HH (1999b) Hydration and lyotropic melting of amphiphilic molecules—a thermodynamic study using humidity titration calorimetry. *J Colloid Interface Sci* 220:235–249
- Binder H, Arnold K, Ulrich AS, Zschörnig O (2000) The effect of Zn^{2+} on the secondary structure of a histidine-rich fusogenic peptide and its interaction with lipid membranes. *Biochim Biophys Acta* 1468:345–358
- Binder H, Arnold K, Ulrich AS, Zschörnig O (2001) Interaction of Zn^{2+} with phospholipid membranes. *Biophys Chem* 90:57–74
- Blume A, Hübner W, Messner G (1988) Fourier Transform infrared spectroscopy of $^{13}\text{C}=\text{O}$ -labeled phospholipids. Hydrogen bonding to carbonyl groups. *Biochemistry* 27:8239–8249
- Büldt G, Gally HU, Seelig J, Zaccai GJ (1979) Neutron diffraction studies on phosphatidylcholine model membranes. I. Head group conformation. *J Mol Biol* 134:673–691
- Caracciolo G, Petrucci M, Caminiti R (2005) A new experimental setup for the study of lipid hydration by energy dispersive X-ray diffraction. *Chem Phys Lett* 414:456–460
- Casal HL, Mantsch HH (1984) Polymorphic phase behaviour of phospholipid membranes studied by infrared spectroscopy. *Biochim Biophys Acta* 779:381–401
- Dluhy RA, Chowdhry BZ, Cameron DG (1985) Infrared characterization of conformational differences in the lamellar phase of 1,3-dipalmitoyl-sn-glycero-2-phosphatidylcholine. *Biochim Biophys Acta* 821:437–444
- Faure C, Bonakdar L, Durfoue EJ (1997) Determination of DMPC hydration in the La and Lb' phases by ^2H solid state NMR D $_2\text{O}$. *FEBS Lett* 405:263–266
- Finer EG, Darke A (1974) Phospholipid hydration studied by deuterium magnetic resonance spectroscopy. *Chem Phys Lipids* 12:1–16
- Fringeli UP, Müldner HG, Günthard HH, Gasche W, Leuzinger W (1972) The structure of lipids and proteins studied by attenuated total reflection (ATR) infrared spectroscopy. I. Oriented layers of tripalmitin. *Z Naturf* 27b:780–796
- Frischleder H, Gleichmann S, Krahl R (1977) Quantum-chemical and empirical calculations on phospholipids. III. Hydration of the dimethylphosphate anion. *Chem Phys Lipids* 19:144–149
- Gawrisch K, Richter W, Möps A, Balgavy P, Arnold K, Klose G (1985) The influence of water concentration on the structure of egg yolk phospholipid/water dispersions. *Stud Biophys* 108:5–16
- Gawrisch K, Ruston D, Zimmerberg J, Parsegian VA, Rand RP, Fuller N (1992) Membrane dipole potential, hydration forces, and the ordering of water at membrane surfaces. *Biophys J* 61:1213–1223
- Grdadolnik J, Kidric J, Hadzi D (1991) Hydration of phosphatidylcholine reversed micelles and multilayers—an infrared spectroscopic study. *Chem Phys Lipids* 59:57–68
- Grdadolnik J, Kidric J, Hadzi D (1994) An FT-IR study of water hydrating dipalmitoylphosphatidylcholine multibilayers and reversed micelles. *J Mol Struct* 322:93–103
- Harrick NJ (1967) Internal reflection spectroscopy. Wiley, New York
- Israelachvili JN, Wennerström H (1996) Role of hydration and water structure in biological and colloidal interactions. *Nature* 376:219–225
- Jendrasia GL, Hasty JH (1974) The hydration of phospholipids. *Biochim Biophys Acta* 337:79–91
- Kamb B (1968) Ice polymorphism and the structure of water. In: Rich A, Davidson N (eds) Structural chemistry and molecular biology. W. H. Freeman, San Francisco, pp 507–542
- Kint S, Wermer PH, Scherer JR (1992) Raman spectra of hydrated phospholipid bilayers. 2. Water and head-group interactions. *J Phys Chem* 96:446–452
- Klose G, Arnold K, Peinel G, Binder H, Gawrisch K (1985) The structure and dynamics of water near membrane surfaces. *Colloids Surf* 14:21–30
- Le Neveu DM, Rand RP, Parsegian VA (1976) Measurement of forces between lecithin bilayers. *Nature* 259:601–603

- Leikin S, Parsegian DC (1993) Hydration forces. *Annu Rev Phys Chem* 44:369–395
- Leikin V, Parsegian VA, Yang WH, Walrafen GE (1997) Raman spectral evidence for hydration forces between collagen triple helices. *Proc Natl Acad Sci USA* 94:11312–11317
- Luzzati V (1968) X-ray diffraction studies of lipid-water systems, vol 1. Academic, London
- McGrath R, Madden WG, Bergren MS, Rice SA, Sceats MG (1978) A theoretical study of the OH-stretching region of the vibrational spectrum of ice Ih. *J Chem Phys* 69:3483–3495
- Milhaud J (2004) New insights into water-phospholipid interactions. *Biochim Biophys Acta* 1663:19–51
- Murphy DM, Koop T (2005) Review of the vapour pressures of ice and supercooled water for atmospheric applications. *QJR Meteorol Soc* 131:1539–1565
- Parsegian VA, Rand RP (1991) On molecular protrusion as the source of hydration forces. *Langmuir* 7:1299–1301
- Parsegian VA, Fuller N, Rand RP (1979) Measured work of deformation and repulsion of lecithin bilayers. *Proc Natl Acad Sci USA* 76:2750–2754
- Pasenkiewicz-Gierula M, Takaoka Y, Miyagawa H, Kitamura K, Kusumi A (1999) Charge pairing of headgroups in phosphatidylcholine membranes: a molecular dynamics simulation study. *Biophys J* 76:1228–1240
- Pasenkiewicz-Gierula M, Rog T, Kitamura K, Kusumi A (2000) Cholesterol effects on the phosphatidylcholine bilayer polar region: a molecular simulation study. *Biophys J* 78:1376–1389
- Peinel G, Binder H, Werge C (1983a) The phospholipid–water interface. A theoretical study. *Stud Biophys* 93:211–214
- Peinel G, Frischleder H, Binder H (1983b) Quantum-chemical and empirical calculations on phospholipids. VIII. The electrostatic potential from isolated molecules up to layer systems. *Chem Phys Lipids* 33:195–205
- Pfeiffer H, Binder H, Klose G, Heremans K (2003a) Hydration pressure and phase transitions of phospholipids—I. Piezotropic approach. *Biochim Biophys Acta* 1609:144–147
- Pfeiffer H, Binder H, Klose G, Heremans K (2003b) Hydration pressure and phase transitions of phospholipids—II. Thermotropic approach. *Biochim Biophys Acta* 1609:148–152
- Pohle W, Selle C, Fritzsche H, Binder H (1998) Fourier transform infrared spectroscopy as a probe for the study of the hydration of lipid self-assemblies. I. Methodology and general phenomena. *Biospectroscopy* 4:267–280
- Rand RP, Parsegian VA (1989) Hydration forces between phospholipid bilayers. *Biochim Biophys Acta* 988:351–376
- Seelig J (1977) Deuterium magnetic resonance: theory and application to lipid membranes. *Q Rev Biophys* 10:353–418
- Ter-Minassian-Saraga L, Okamura E, Umemura J, Takenaka T (1988) Fourier transform infrared-attenuated total reflection spectroscopy of hydration of dimyristoylphosphatidylcholine multibilayers. *Biochim Biophys Acta* 946:417–423
- Vedamuthu M, Singh S, Robinson GW (1994) Properties of liquid water: origin of density anomalies. *J Phys Chem* 98:2222–2230
- Walrafen GE (1967) Raman spectral studies of the effects of temperature on water structure. *J Chem Phys* 47:114–127
- Walrafen GE (1971) Raman spectral studies of the effects of solutes and pressure on water structure. *J Chem Phys* 55:768–792
- Walrafen GE, Chu YC (1995) Linearity between structural correlation length and correlated proton Raman intensity from amorphous ice and supercooled water up to dense supercritical steam. *J Phys Chem* 99:11225–11229
- Yegiazaryan GA, Poghosyan AH, Shahinyan AA (2006) The water molecules orientation around the dipalmitoylphosphatidylcholine head group: a molecular dynamics study. *Physica A* 362:197–203
- Zhou F, Schulten K (1995) Molecular dynamics study of a membrane–water interface. *J Phys Chem* 99:2194–2207
- Zundel G (1969) Hydration and intermolecular interactions. Academic, New York